International Journal of Engineering Technology and Management Sciences
Website: ijetms.in Issue: 5 Volume No.7 September - October – 2023
DOI:10.46647/ijetms.2023.v07i05.023 ISSN: 2581-4621

# ACTIVE VOLTAGE CONTROL OF DFIG BASED ON WIND FARM POWER SYSTEM

**Ram Krishan Kumar*[1], Jayanti choudhary[2]**
[1]Research scholar, National Institute of Technology Patna (800005) India
[2]Assistant professor, National Institute of Technology Patna (800005) India

**Abstract**
We know that large-scale wind farms are commonly integrated with long-distance transmission systems. This paper is about doubly-fed induction generators with wind farm systems and the access point voltage of doubly-fed induction generators undergoes a stability problem, due to the variation in speed of the wind. Hence, the reactive power capability of the wind farm and the reactive power demand of the system are studied with the help of decoupled controllable control, maintaining the access point voltage irrespective of the variations in the speed of the wind.

## 1. Introduction: -

Today, the wind industry is becoming one of the world's fastest-growing energy markets, helping to meet worldwide energy needs. Due to their benefits such as variable speed constant frequency operation, decreased flicker, and independent control capabilities for active and reactive forces, wind turbines based on doubly fed induction generators have attracted special attention [1]. The generator's active power is determined by the turbine control and of course, must be within the capacity of the turbine generator system [2-3].

Apparently, a Doubly Fed Induction Generator is a wound rotor induction system consisting of back-to-back power converters. There are two converters connected back-to-back on the rotor side with the help of a DC link.

One of the power converters which is on the grid side is known as a grid controller. The main objective of the grid-side converter is to keep the DC-link voltage constant [4-6].

Another power converter that is used on the rotor side is known as the rotor controller. Rotor controllers are used to govern the power fed into that rotor.

At sub-synchronous and super-synchronous rates, DFIM can act as a motor as well as a generator. This operation is called a super-synchronous operation when the computer operates above synchronous speed. Likewise, sub-synchronous operation is termed operation below synchronous speed. The unit can be run either as a motor or a generator in both sub- and super-synchronous operations.

In this type of generator, managed power electronic converters are used to increase performance, DFIG are variable speed generators with benefits than others, they are being used more in wind turbines because their control is simpler energy efficiency is higher than some other generators, and power quality is enhanced.

some important factor

A. On DC side analysis

Voltage ripple factor (Vrf):- It is measured on harmonic on the DC side of the converter.

$$\text{Vrf} = \sqrt{F \cdot F^2 - 1} \quad (1)$$

$$\text{F.F} = \text{Form factor} = \text{Vor} / \text{Vo} \quad (2)$$

Where

Vor = R.m.s value of voltage

DOI:10.46647/ijetms.2023.v07i05.023 ISSN: 2581-4621

Vo = Avg. Value of voltage
The form factor is always greater than 1.
When F.F = 1 then it indicates the pure DC source without any harmonic present.
When F.F >1 Then it indicates dc source with harmonic

B. On an ac side analysis

Total harmonic distortion (T.H.D) = $\sqrt{\frac{1}{g^2}-1}$ (3)

Where
g = Distortion factor
Total harmonic distortion = it is a measure of harmonic on ac side of the converter.

Distortion factor (g) = to understand the smoothness of the wave on ac side.
g is always less than equal to 1.
When g = 1 then T.H.D = 0
So, no harmonic present on ac side.
When g<1 then it indicates some harmonic present on a side

**2. Electrical circuit**
2.1 Dynamic model

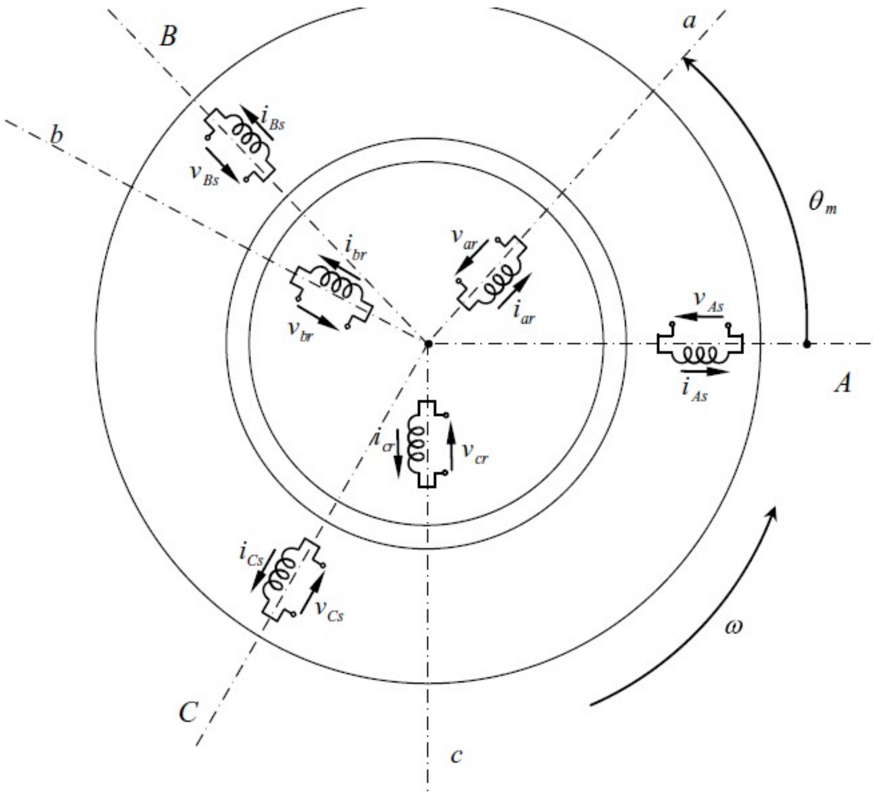


Figure 1. Ideal three phase winding of DFIG

According to the model of AC machines developed by the simplified and idealized DFIG perfect model can be described as three winding in the stator and three winding in the rotor which is shown above in Figure 1 [6-7].

Such winding is a perfect reflection of the actual machine that enables. Derive an electrical circuit equivalent, as seen in Figure 2.

Website: ijetms.in Issue: 5 Volume No.7 September - October – 2023
DOI:10.46647/ijetms.2023.v07i05.023 ISSN: 2581-4621

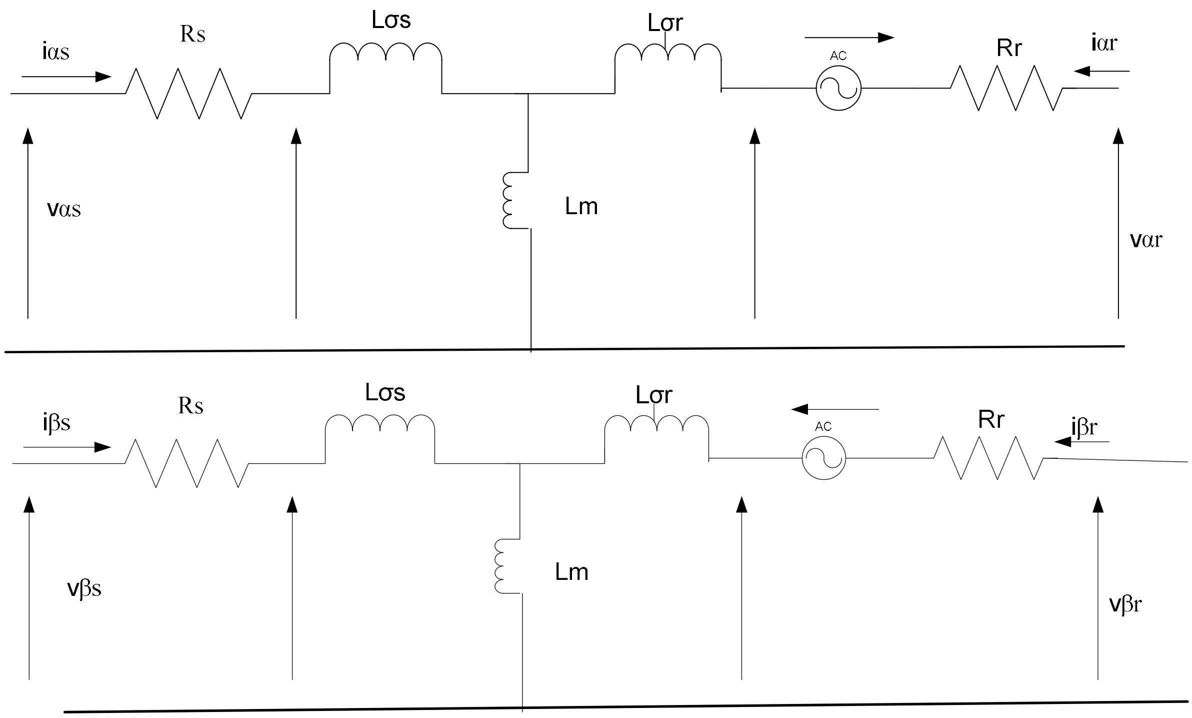


Figure 2. $\alpha - \beta$ model of DFIM in stator coordinates.

The DFIG voltage equations in space vector form.

$$\overset{\to S}{V_S} \equiv R_S \overset{\to s}{i_s} + \frac{d\overset{\to s}{\psi_s}}{dt} \tag{4}$$

$$\overset{\to r}{V_r} \equiv R_r \overset{\to r}{i_r} + \frac{d\overset{\to r}{\psi_r}}{dt} \tag{5}$$

Equation (4) represented in stator coordinates or in $\alpha - \beta$ reference frame and equation (5) represented in rotor coordinates or $D$-Q reference frame. ‘s’ and ‘r’ indicates the referred vectors of the stator reference frame and the rotor reference frame respectively [8-13].

Similar to this, in space vector notation, the correlation between the current and the flux is...

$$\overset{\to s}{\psi_s} \equiv L_S \overset{\to s}{i_s} + L_m \overset{\to s}{i_s} \tag{6}$$

$$\overset{\to r}{\psi_r} \equiv L_r \overset{\to r}{i_r} + L_m \overset{\to r}{i_s} \tag{7}$$

$$L_s \equiv L_{\sigma s} + L_m \tag{8}$$

$$L_r \equiv L_{\sigma r} + L_m \tag{9}$$

With the help of coordinate transformation equation (6), equation (7) is represented in stator and rotor reference frames respectively.

$$\overset{\to s}{\psi_s} \equiv L_s \overset{\to s}{i_s} + L_m \overset{\to s}{i_r} \equiv L_S \overset{\to s}{i_s} + L_m e^{j\theta_m} \overset{\to r}{i_r} \tag{10}$$

$$\overset{\to r}{\psi_r} \equiv L_r \overset{\to r}{i_r} + L_m \overset{\to r}{i_s} \equiv L_r \overset{\to r}{i_r} + L_m e^{-j\theta_m} \overset{\to s}{i_s} \tag{11}$$

Multiplying the equation (10) by $e^{j\theta_m}$ for transforming the corresponding space vector to the frame of the stator reference, the $\alpha - \beta$ model of DFIG is obtained in stator coordinates which is shown below: -

$$\overset{\to s}{V_s} \equiv R_s \overset{\to s}{i_s} + \frac{d\overset{\to s}{\psi_s}}{dt} \tag{12}$$

$$\overset{\to s}{V_r} \equiv R_r \overset{\to s}{i_s} + \frac{d\overset{\to s}{\psi_r}}{dt} \text{-j}\omega_m \overset{\to s}{\psi} \tag{13}$$

$$\overset{\to s}{\psi_s} \equiv L_s \overset{\to s}{i_s} + L_m \overset{\to s}{i_r} \tag{14}$$

$$\overset{\to s}{\psi_r} \equiv L_r \overset{\to s}{i_r} + L_m \overset{\to s}{i_s} \tag{15}$$

DOI:10.46647/ijetms.2023.v07i05.023 ISSN: 2581-4621

$$\because \frac{d\vec{\psi}_r^r}{dt} e^{j\theta_m} \equiv \frac{d\left(\vec{\psi}_r^r e^{j\theta_m}\right)}{dt} \text{-j}\omega_m \vec{\psi}_r^r e^{j\theta_m}$$

$$and \quad \vec{\psi}_{\cdot s}^{s} \equiv \left(\vec{\psi}_r^r e^{j\theta_m}\right)$$

$$P_s \equiv \frac{3}{2} Re\{\vec{v}_s \vec{i}_s^{*}\} \equiv \frac{3}{2}\{v_{\alpha s}.i_{\alpha s} + v_{\beta s}.i_{\beta s}\} \quad (16)$$

$$P_r \equiv \frac{3}{2} Re\{\vec{v}_r \vec{i}_r^{*}\} \equiv \frac{3}{2}\{v_{\alpha r}.i_{\alpha r} + v_{\beta r}.i_{\beta r}\} \quad (17)$$

$$Q_S \equiv \frac{3}{2} Im\{\vec{v}_s \vec{i}_s^{*}\} \equiv \frac{3}{2}\{v_{\beta s}.i_{\beta s} - v_{\alpha s}.i_{\alpha s}\} \quad (18)$$

$$Q_r \equiv \frac{3}{2} Im\{\vec{v}_r \vec{i}_r^{*}\} \equiv \frac{3}{2}\{v_{\beta r}.i_{\beta r} - v_{\alpha r}.i_{\alpha r}\} \quad (19)$$

The electromagnetic torque expression gets as follow: -

$$T_{em} \equiv \frac{3}{2} p.Im\{\vec{\psi}_r.\vec{i}_r^{*}\} \equiv \frac{3}{2} p\left(\psi_{\beta r} i_{\alpha r} - \psi_{\alpha r} i_{\beta r}\right) \quad (20)$$

$$T_{em} \equiv \frac{3}{2} p.\frac{L_m}{L_s} Im\{\vec{\psi}_s.\vec{i}_r^{*}\} \equiv T_{em} \equiv \frac{3}{2} p.Im\{\vec{\psi}_s^{*}.\vec{i}_s\}$$

$$\equiv \frac{3}{2} p.\frac{L_m}{L_r} Im\{\vec{\psi}_r^{*}.\vec{i}_s\}$$

$$\equiv \frac{3}{2} p.\frac{L_m}{\sigma L_r L_s} Im\{\vec{\psi}_r^{*}.\vec{\psi}_s\}$$

$$\equiv \frac{3}{2} L_m p.Im\{\vec{i}_s \times \vec{i}_r^{*}\}$$

$$\sigma \equiv 1 - \frac{{L_m}^2}{L_s L_r}$$

$$\equiv Leakage - coeficien$$

### 3. Control for Extraction of optimal Power

According to the frame of reference in synchronous rotation, the models of the DFIG on stator and rotor side are provided which are shown below: -

$$u_{sd} = R_s i_{sd} + \frac{d\psi_{sd}}{dt} - \omega_s \psi_{sq}$$

$$u_{sq} = R_s i_{sq} + \frac{d\psi_{sq}}{dt} + \omega_s \psi_{sd} \quad (21)$$

$$u_{rd} = R_r i_{rd} + \frac{d\psi_{rd}}{dt} - \omega_{s1} \psi_{rq}$$

$$u_{rq} = R_r i_{rq} + \frac{d\psi_{rq}}{dt} + \omega_{s1} \psi_{rd} \quad (22)$$

$$\psi_{sd} = L_s i_{sd} + L_m i_{rd}$$

$$\psi_{sq} = L_s i_{sq} + L_m i_{rq} \quad (23)$$

$$\psi_{rd} = L_r i_{rd} + L_m i_{sd}$$

$$\psi_{rq} = L_r i_{rq} + L_m i_{sq} \quad (24)$$

As follows are the terms for the stator's active and reactive power:

$$P_s = - u_{sd} i_{sd} - u_{sq} i_{sq}$$

$$Q_s = u_{sd} i_{sq} - u_{sq} i_{sd} \quad (25)$$

When d-axis is aligned with voltage vector of the stator, neglecting the stator resistance and we are considering.

$$u_{sd} = U_s$$

$$u_{sq} = 0 \,, \quad R_s = 0 \,, \ \psi_{sd} = 0 \ , \psi_{sq} = \psi_s$$

$$\psi_s = \frac{-U_S}{\omega_s}$$

International Journal of Engineering Technology and Management Sciences
Website: ijetms.in Issue: 5 Volume No.7 September - October – 2023
DOI:10.46647/ijetms.2023.v07i05.023 ISSN: 2581-4621

$$\frac{d\psi_s}{dt} = 0 \tag{26}$$

$$i_{sd} = \frac{-L_m i_{rd}}{L_s}$$

$$i_{sq} = \frac{(\psi_s - L_m i_{rq})}{L_s} \tag{27}$$

Substituting equation (24), (25) and (27) into equation (22) then we get

$$(di\_rd)/dt = 1/(\sigma L\_r)(u_{rd} - R_r i_{rd} + \omega_{s1}\sigma L_r i_{rq} - \frac{\omega_{s1L_m\psi_s}}{L_s}$$

$$(di\_rq)/dt = 1/(\sigma L\_r)(u_{rq} - R_r i_{rq} - \omega_{s1}\sigma L_r i_{rd} \tag{28}$$

$$\sigma = 1 - \frac{{L_m}^2}{L_s L_r}$$

Now simplified active and reactive power of the stator.

$$P_s =- u_{sd} i_{sd} = \frac{u_s L_m i_{rd}}{L_s}$$

$$Q_s = u_{sd} i_{sq} = \frac{u_s(\psi_s - L_m i_{rq})}{L_s} \tag{29}$$

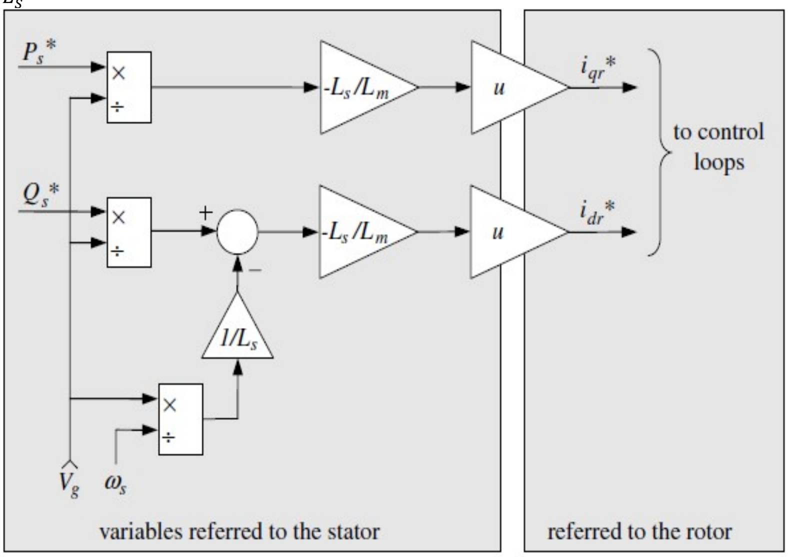


Figure 3. current reference control

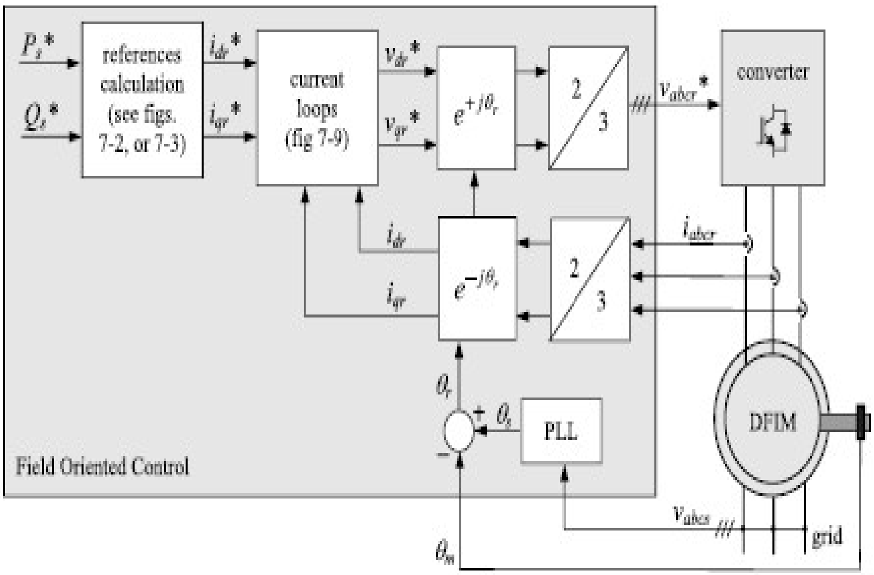


Figure 4. schematic diagram of vector control system

International Journal of Engineering Technology and Management Sciences
Website: ijetms.in Issue: 5 Volume No.7 September - October – 2023
DOI:10.46647/ijetms.2023.v07i05.023 ISSN: 2581-4621

## 4. Simulation Circuit

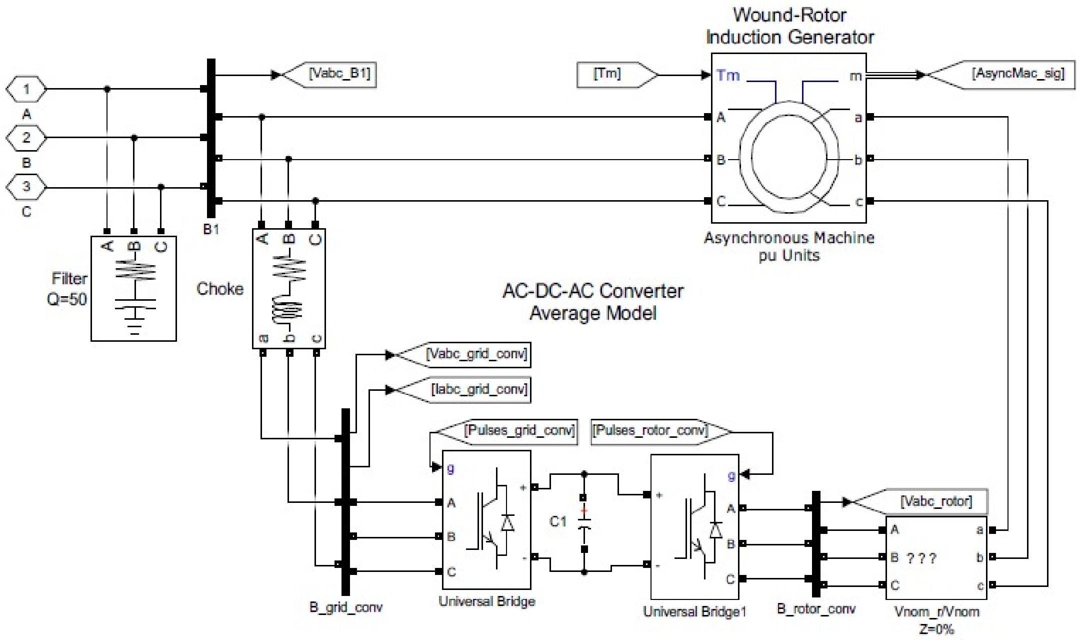


Figure 5. Simulation circuit.

## 5. simulation result

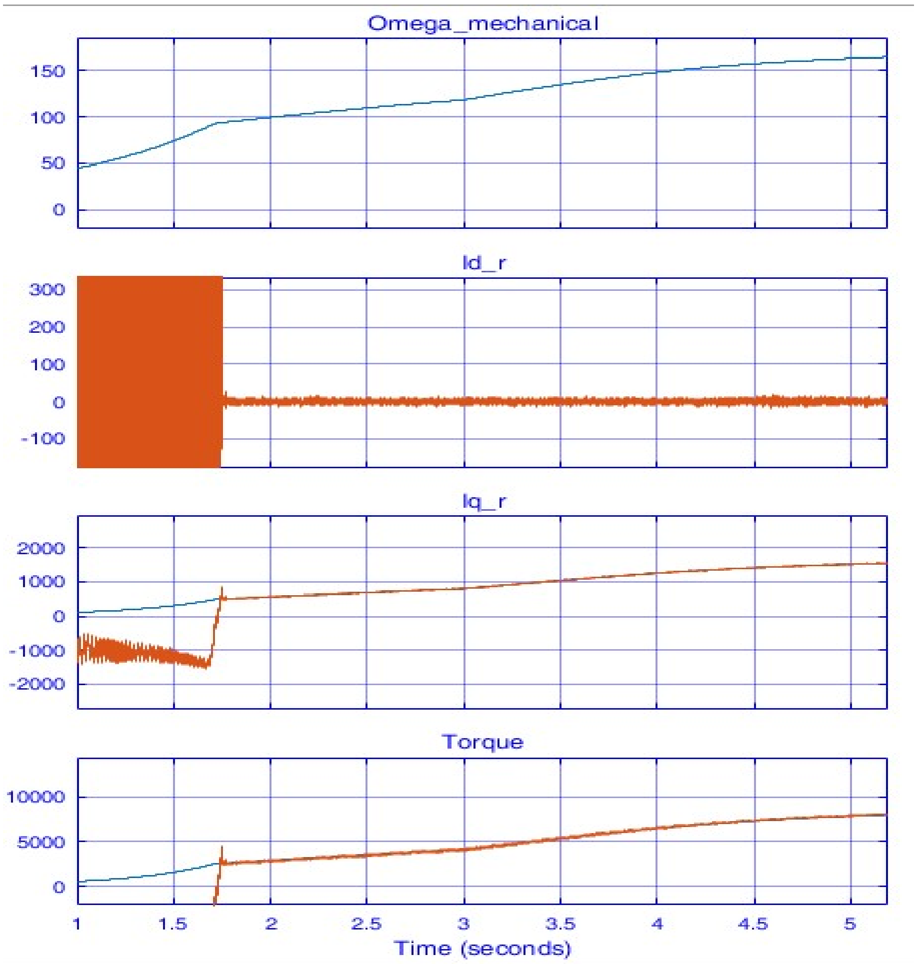

DOI:10.46647/ijetms.2023.v07i05.023 ISSN: 2581-4621

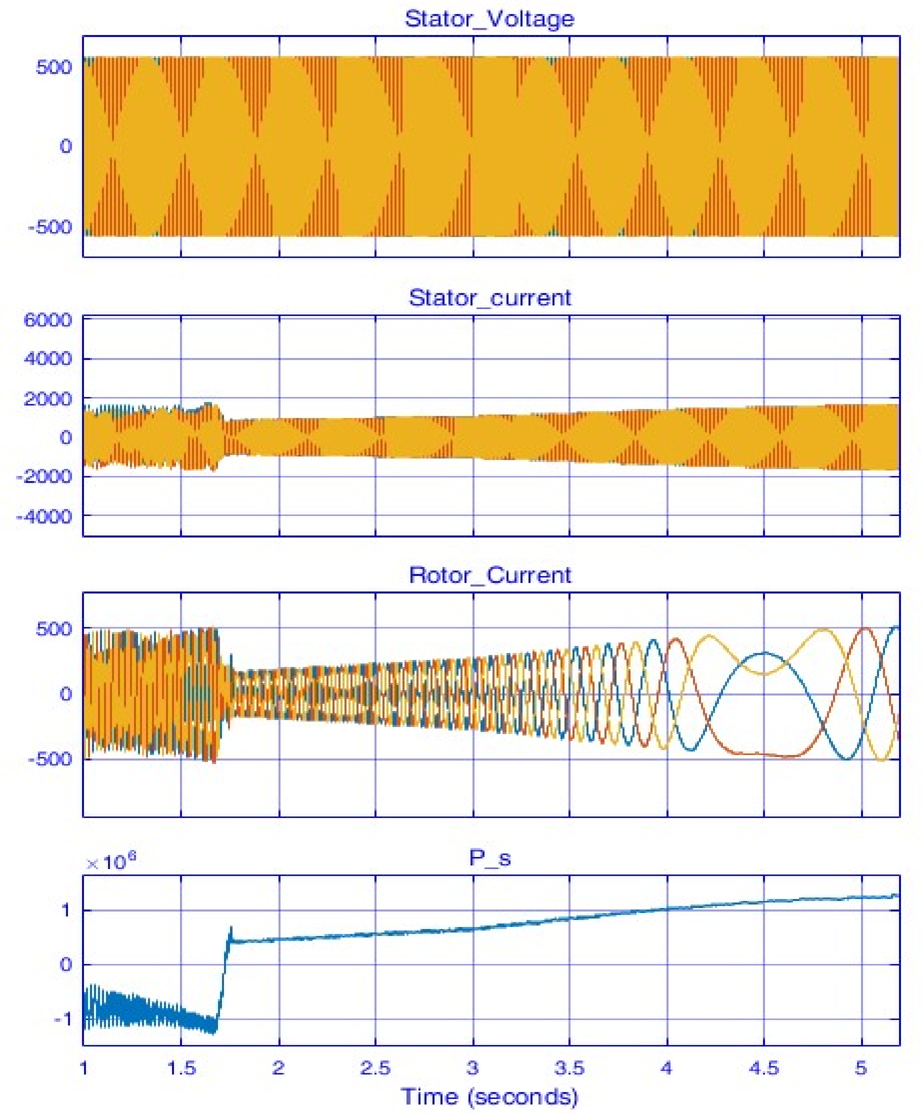


Figure 6. simulation result of DFIG.

## 6. Conclusion

The DFIG-based WECS mathematical model is presented first. The active voltage of the stator of DFIG is to be maintain a constant value irrespective the variation in the speed of the wind. so, it is most useful idea to generate synchronized power at constant voltage either change in mechanical input due to the change in wind speed.

## 7. References: -

[1]. Sudipta Ghosh*, Member, IEEE*, Younes J. Isbeih*, Member, IEEE*, Rojan Bhattarai*, member, IEEE*,Mohamed Shawky El Moursi*, Senior Member, IEEE*, Ehab F. El-Saadany *, Fellow, IEEE*, and Sukumar Kamalasadan*, Senior Member, IEEE. "*A Dynamic Coordination Control Architecture for Reactive Power Capability Enhancement of the DFIG-Based Wind Power Generation." IEEE transactions on power systems, Vol. 35, No.4, July 2020.

[2]. Hailiang Xu 1, (Member, IEEE), Yufeng Zhang 1, Zhi Li1, Rende Zhao 1,and Jiabing Hu2, (Senior Member, IEEE). "Reactive Current Constraints and Coordinated Control of DFIG's RSC and GSC During Asymmetric Grid Condition." Received September 9, 2020, accepted October 1, 2020, date of publication October 7, 2020, date of current version October 20, 2020.

[3]. Ruo Huan Yang, student member, IEEE, and Jian Xun Jin, senior Member, IEEE."Unified Power Quality Conditioner with advanced dual control for performance improvement of DFIG-Based wind farm". IEEE transactions on sustainable energy, Vol.12, No. 1, January 2021.

[4]. L. Zhang, T.Ye, andY. Xin, "Problems and measures of power grid accommodating large scale wind power," *Proc. CSEE*, vol. 30, no. 25, pp. 1–9, Sep. 2010.

[5]. Q. Guo, H. Sun, and B.Wang, "Hierarchical automatic voltage control for integration of large-scale wind power: Design and implementation," *Elect. Power Syst. Res.*, vol. 120, no. 120, pp. 234–241, Mar. 2015.

[6]. M. Thompson, T. Martini, and N. Seeley, "Volt/VAR control for wind generation," in *Proc. IEEE PES Transmiss. Distrib. Conf. Expo.*, 2012, pp. 1–5.

[7]. S. Abulanwar, W. Hu, F. Iov, and Z. Chen, "Adaptive voltage control strategy for variable-speed wind turbine connected to a weak network," *IET Renewable Power Gener.*, vol. 10, no. 2, pp. 238–249, Feb. 2016.

[8]. A. K. Pathak, M. P. Sharma, and M. Bundele, "A critical review of voltagen and reactive power management of wind farms," *Renewable Sustain. Energy Rev.*, vol. 51, pp. 460–471, Nov. 2015.

[9]. X. Ye, Y. Qiao, and Z. Lu, "Cascading tripping out of numerous wind turbines in China: Fault evolution analysis and simulation study," in *Proc. IEEE PES Gen. Meeting*, 2012, pp. 1–11.voltage control for DFIG based wind farm," *Proc. CSEE*, vol. 32, no. 19, pp. 16–23, Jul. 2012.

[10]. M. E. Moursi, G. Joos, and C. Abbey, "A secondary voltage control strategy for transmission level interconnection of wind generation," *IEEE Trans. Power Electron.*, vol. 23, no. 3, pp. 1178–1190, May 2008.

[11]. G. Tapia, A. Tapia, and J. X. Ostolaza, "Proportional–integral regulatorbased approach to wind farm reactive power management for secondary voltage control," *IEEE Trans. EnergyConvers.*, vol. 22, no. 2, pp. 488–498, Jun. 2007.

[12]. J. Mart´ınez, P. Kjaer, P. Rodriguez, and R. Teodorescu, "Design and analysis of a slope voltage control for a DFIG wind power plant," *IEEE Trans. Energy Convers.*, vol. 27, no. 1, pp. 11–20, Mar. 2012.

[13]. Y. Li, Z. Xu, and J. Zhang, "Variable droop voltage control for wind farm," *IEEE Trans. Sustain. Energy*, vol. 9, no. 1, pp. 491–493, Jan. 2017.